Column separation with the effect of air release in viscoelastic pipes

H.A. Warda, H.A. Kandil, A.A. Elmiligui, and E.M. Wahba

Mechanical Eng. Dept., Faculty of Eng., Alexandria University, Alexandria 21544, Egypt

In this study, a numerical model based on the Method Of Characteristics (MOC) is developed for modeling pressure transients in viscoelastic pipelines in the presence of column separation. The model is capable of modeling complex phenomena, which could not be modeled by the standard MOC, such as unsteady friction and viscoelastic behavior of the pipe walls. Unsteady friction is modeled through a universal model developed by the authors. The viscoelastic behavior of the pipe walls is modeled through a one-element Kelvin-Voigt Viscoelastic Model. The column separation phenomenon is simulated through two models; namely the Discrete Vapor Cavity Model (DVCM) and the Discrete Gas Cavity Model (DGCM). In comparison with the DVCM, the DGCM was shown to enable a better prediction of the pressure transients in the system. An expression was developed for the effective wave speed in the DGCM and this expression was compared with the expression of the wave speed for two-phase flow transients of low void fraction. However, the rate of gas release assumed in the DGCM, remains a highly sensitive parameter in the model. An experimental setup was constructed to provide reliable experimental data for transient flows in PVC (viscoelastic) pipes to verify the numerical model. Eventually, the numerical model was experimentally verified to be capable of dealing with all unsteady complex phenomena and efficiently simulating the pressure transients in the presence of column separation.

فى هذه الدراسة تم تطوير نموذج عددى مبنى على طريقة الخصائص ليكون قادرا على محاكاة الضغوط العابرة فى الأنابيب ذات المرونة اللزجة فى حالة انفصال عامود السائل. هذا النموذج قادر على التعامل مع موضوعات متخصصة مثل تأثير الاحتكاك غير المستقر و المرونة اللزجة لجدران الأنابيب على الضغوط العابرة. علما بأن طريقة الخصائص القياسية لا تستطيع التعامل مع هــذه الظواهــر ممــا يؤدى إلى عدم قدرتها على محاكاة الموجات التضاغطية التى تتولد فى الأنابيب خاصة بعد مرور الموجة التضاغطية الأولى. تمت محاكاة الاحتكاك غير المستقر فى الأنابيب باستخدام نموذج شامل تم تطويره بواسطة الباحثين الحاليين و يمكن استخدامه فى جميع أنماط السريان من سريان طبقي إلى سريان اضطرابي كما تمت محاكاة المرونة اللزجة لجدران الأنابيب مــن خــلال نمــوذج كيلفن-فويجت ذو عنصر واحد. تمت محاكاة ظاهرة انفصال عامود السائل من خلال نموذجين هما نموذج الـتجويف الـبخاري المنفصـل ونموذج التجويف الغازي المنفصل. بالمقارنة بالنتائج المعملية اتضح أن نموذج التجويف الغازي المنفصل قادر على عمل محاكاة أفضل للضغوط العابرة في الأنابيب. تم أيضا تطوير معادلة لسرعة الموجة المعدلة فى نموذج التجويف الغازي المنفصل. تم أيضا توضيح أهمية القيمة المفروضة لكمية الغاز المنبعث كمتغير هام في النموذج. تم إنشاء جهاز معملــى لتوفــير نتائج معملية دقيقة للسريان العابر في الأنابيب ذات المرونة اللزجة للتحقق من صحة النموذج الرقمي المستخدم. وبالتالي تم التحقق من قدرة النموذج على محاكاة السريان العابر في الأنابيب آخذا في الاعتبار تأثير جميع الظواهر السابق ذكرها.

Keywords: Column separation, Unsteady friction, Air release, Viscoelastic pipes

1. Introduction

Hydraulic transients through piping systems produce periodic pressure variation at any point of the pipe. The period of oscillations depends on the wave speed and the distance between the reflectors (boundaries). Two important phenomena disrupt this orderly view of the transient, both of which are related to the occurrence of low pressures. The first of them is the release of the dissolved air (gas) when the pressure falls below its release level

and the second is the formation of vapor cavities in the pipe when the pressure falls to the liquid vapor pressure, a phenomenon well known as column separation. These two phenomena are usually interrelated.

Pressure transients occur in any fluid system subjected to changes in flow conditions. Therefore, an accurate monitoring of the pressure transients through a well-developed numerical model is a necessity for design engineers. This study is concerned with developing a numerical model for studying the

pressure-transient propagation within fluid systems in viscoelastic pipes in the presence of column separation.

The initial step is to consider the standard MOC. It is noticed that the studies covering the application of the MOC to unsteady flow problems developed continuously over the last 50 years. For example, Watters [1] provided the detailed theoretical basis for estimating the wave speed in different types of conduits. Also, Wylie and Streeter [2] summarized the various methods of solution for the water hammer problem. They concluded that the MOC is considered to be the standard numerical method by which other methods may be judged for accuracy and efficiency in modeling pressure transients.

Kaplan et al. [3] showed that transients arising in long oil pipelines could be adequately simulated by the MOC. On the other hand, Bergant and Simpson [4] demonstrated the numerical inaccuracies that could arise from applying the standard MOC when a solution is needed at the boundaries such as valves, orifices and centrifugal pumps. Also, Boulos et al. [5] presented a basis for verifying the accuracy of numerical techniques applied to transient flow in pipe systems.

In applying the standard MOC, a noticeable distortion was observed between the experimental data and the results of the numerical model. This is because the standard MOC is not capable of modeling complex phenomena such as unsteady friction, viscoelasticity of the pipe walls and the probable occurrence of column separation.

One objective of the present study is to modify the MOC for accurate and efficient modeling of these complex phenomena. First, the unsteady friction was considered where the existing models were reviewed, tested and modified in order to develop a universal model to be used in the MOC for accurate modeling in all flow regimes.

Among the models developed by previous investigators for unsteady friction are those by Zeilke [6], for laminar flows, and by Vardy and Hwang [7] and Brunone et al. [8] for turbulent flows.

Zielke [6] developed a weighting-function model, for friction losses in transient laminar flow in pipes, based on an exact analytical solution of laminar flow equations. Later,

Zielke's model was greatly modified by Trikha [9]. Also, Suzuki et al. [10] presented an alternative approach for improving Zielke's weighting function model for laminar flow of liquids in pipes.

Vardy and Hwang [7] developed a weighting function model for transient turbulent pipe friction at moderate Reynolds numbers. Another weighting-function model for transient turbulent friction in smooth pipes was later developed by Vardy and Brown [11].

A third unsteady-friction model was developed by Brunone et al. [8] for turbulent flows. Brunone et al. [12] introduced a modified characteristic method where the unsteady friction is modeled through a new term added to the usual equations of the MOC and evaluated in an explicit manner.

Each of the above three unsteady-friction models were tested by the authors [13] for both laminar and turbulent flow cases. It was shown that none of the models could be used accurately and efficiently for both laminar and turbulent flows. A universal model was proposed by introducing a modification to Vardy et al.'s model [7], originally developed for turbulent flow, to make it suitable for laminar flows. The modified model was experimentally verified [13] to be capable of modeling unsteady friction in elastic pipes for both laminar and turbulent flow cases. The results showed that unsteady friction has a minor effect on damping the pressure transients in viscoelastic pipes while it has a dominant damping effect in elastic pipes. The next step was to modify the numerical model to account for the viscoelastic effects of the pipe walls.

It is noted that the methods used by previous investigators to model the viscoelastic effects may be divided into two categories; the first is based on the MOC while the second is based on frequency-response method.

According to Suo and Wylie [14], Rieutord and Blanchard (1979) applied the MOC to study the effect of the viscoelastic behavior of the pipe walls on the transients. Guney [15] studied the pressure transients created by closing a valve at the downstream end of a viscoelastic pipe. He proposed a modified MOC model that takes into account the effects of time-varying diameter and thickness.

However, his model does not include any modeling for unsteady friction in turbulent flow. Also, the model was not verified against experimental data for turbulent flow.

Pezzinga and Scandura [16] proposed the reduction of unsteady flow oscillations by inserting additional pipes of High-Density PolyEthylene (HDPE) at the upstream end of the pipeline in a pumping installation. The mechanical behavior of the HDPE is described by both a linear elastic model and a Kelvin-Voigt viscoelastic model. The results of the mathematical model were in excellent agreement with the experimental data, even with only one Kelvin-Voigt element.

Warda et al. [17] studied the pressure transients in viscoelastic pipes in the presence of unsteady friction. They used a universal model for unsteady friction [13] while the viscoelastic behavior of the pipe wall was modeled through a one-element Kelvin-Voigt-Viscoelastic model that resulted in good agreement with the experimental data. The viscoelastic effects were shown to be the dominant damping factor of the pressure oscillations in transient flows through pipes exhibiting a viscoelastic behavior. The numerical model presented and experimentally verified by Warda et al. [17] is used in the present study in modeling the pressure transients in viscoelastic pipes.

Finally, the numerical model has to be modified to be capable of modeling the column separation in the presence of air release.

Among the existing models for column separation, as presented by Swaffield and Boldy [18], are the Discrete Vapor Cavity Model (DVCM) and the Discrete Gas Cavity Model (DGCM). The DVCM was introduced by Streeter (1969), as reported by Simpson and Bergant [19]. The model allows vapor cavities to form at computing sections in the MOC. In applying the model, a constant wave speed is assumed for the liquid between computational sections. The DVCM was modified by Safwat and Van der Polder [20] to allow discrete vapor cavities to form at predetermined locations (valves and high points). The modified DVCM eliminates the unrealistic pressures that occurs in the standard DVCM.

The Discrete Gas Cavity Model (DGCM) was introduced by Provoost and Wylie [26] and Wylie [25], according to Simpson and Bergant

[19]. The DGCM takes into account the effect of air release on the column separation phenomenon. This model lumps the mass of free air at computing sections. Each isolated small volume of air expands and contracts isothermally as the pressure varies in accordance with the perfect gas law. Between each computing section, pure liquid is assumed without free air.

Rongqiso and Youhus [21] developed a numerical model for transient cavitation and column separation based on the homogeneous model of two-phase flow. Consistent coincidence has been obtained between the numerical results and the experimental data. However, errors in the value of the pressure peaks were still noticeable. They attributed these discrepancies to the uncertainty of the gas release rate and the difficulty to predict the friction losses during a transient process.

Aga et al. [22] studied the column separation in pipelines due to pump shutdown and/or valve closure. Both water and crude oil were used in the tests. The experiments showed that the pressure history was less irregular for crude oil than for water. The experiments revealed further that the hydrocarbon gases released during separation in crude oil were not significantly absorbed after the separation.

Streeter [25] developed a method for modeling transient cavitating pipe flow. He described the manner in which a rarefaction wave moves through a fluid causing vapor formation, and the equations for vaporous velocity and vapor fraction as functions of distance and time were developed. The MOC was utilized for reaches having no vapor. However, Streeter mentioned that the procedure is too complex to be incorporated into a general program.

Simpson and Wylie [25] investigated water hammer pressures in a pipeline due to the collapse of a vapor cavity adjacent to a valve. They found that short-duration pressure pulses result from the superposition of the valve-closure water-hammer wave and the wave generated by the collapse of the vapor cavity.

Another model was developed by Guney [15] for column separation in viscoelastic pipe. However, the model developed by Guney was not verified against experimental data

involving column separation. The model doesn't include any modeling for unsteady friction in turbulent flow and it was not verified against turbulent-flow experimental data. Also, the model is not capable of dealing with column separation accompanied with release of air.

Simpson and Bergant [19] performed a numerical comparison between six pipe column-separation models. They concluded that the use of the DGCM is recommended for modeling column separation rather than the DVCM or one of its variations.

From the previous review, it is noted that no modified MOC model has been verified experimentally to be capable of modeling the pressure transients in viscoelastic pipes in the presence of column separation and unsteady friction. Therefore, the numerical model to be developed in the present study has to achieve this goal through the following steps:

1) The unsteady friction and the viscoelastic behavior of the pipe walls are accurately modeled.

2) Two column-separation models are used and compared for efficient simulation of the column separation phenomenon and the possible occurrence of air release.

3) Extensive experimental work was performed to produce reliable experimental data for verifying the modified numerical model.

In the following sections, the experimental setup and the governing equations are presented. Then, the numerical results are presented and compared with the experimental measurements.

2. Experimental setup

An experimental setup was constructed in the Fluid Mechanics Lab. at the Faculty of Engineering, Alexandria University for providing reliable experimental data for the verification of the numerical model. The setup is schematically shown in fig. 1. The setup consists of the following main parts:

1) A constant-head, 9-cubic-meter-capacity tank, which is installed on the roof of the laboratory. The tank holds a maximum head of 11 meters above the pipe centerline. A centrifugal pump continuously feeds the tank with water to maintain a constant surface

level. The tank is connected via a 10 cm diameter vertical pipe to a smaller tank (ground tank) of 0.2 cubic meters capacity.

2) A PVC pipe of 25.4-mm. inside diameter, 4.2-mm. thickness and 25.6-m. length. The water flow rate through the PVC pipe could be controlled using a gate valve. The flow rate is measured using a calibrated tank and a stopwatch.

3) A normally closed solenoid-operated valve with a closure time of 0.08 seconds.

4) Measuring, monitoring and recording equipment that include: two piezoelectric pressure transducers mounted on the PVC pipe at locations 0.03 m and 15.3 m upstream of the solenoid valve. Each transducer is connected to a one-channel charge amplifier (Type 5011). The charge amplifier is responsible for converting the electric charge produced by the piezoelectric transducer into a proportional voltage signal. The output signal from the charge amplifier is then transmitted to a LeCroy (Type 6810) waveform recorder that converts analog waveforms into digital data. The signal recorded by the waveform recorder is then transferred to a personal computer through a GPIB interface card. Software packages are then used to display and analyze the recorded pressure data.
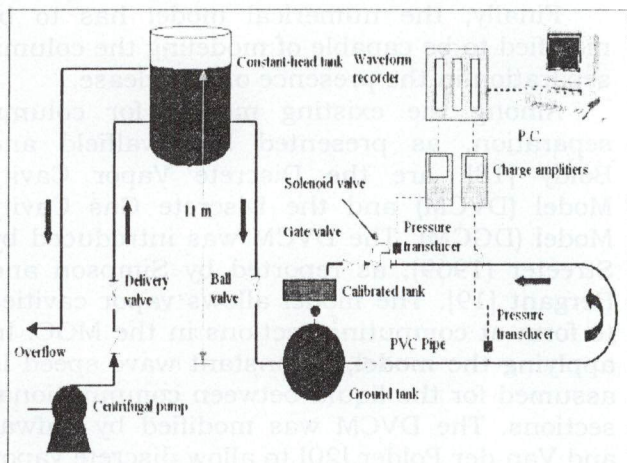

Fig. 1. Diagrammatic sketch of the experimental setup.

2.1. Experimental test cases

The test cases summarized in the following table were performed using a test pipe of a

length of 25.6 m, an inside diameter of 0.0254 m and a wall thickness of 0.0042 m.

Test case no.	1	2	3	4	5
Steady state velocity, V (m/s)	0.062	0.233	0.285	2.2695	0.0235
Reynolds number, R_N	1575	5918	7239	57150	597
Coefficient of friction, f	0.04	0.035	0.032	0.03	0.107

In test cases (1) to (4) measurements were taken at the valve only while in test case (5) measurements were taken at both the valve and a point 15.3-m upstream of the valve. The results of test case (4), where column separation was present, were used to verify the column separation models. Test cases (1,2,3 and 5) were used to verify other models such as the unsteady friction model and the viscoelastic model [13, 17].

3. Governing equations

3.1. Standard MOC

The governing equations are given by Watters [1] as follows:

Continuity equation;

$$\frac{1}{\rho}\frac{dP}{dt} + a^2\frac{\partial V}{\partial s} = 0.$$

(1)

Euler (momentum) equation;

$$\frac{dV}{dt} + \frac{1}{\rho}\frac{\partial P}{\partial s} + g\frac{dz}{ds} + \frac{f}{2D}V|V| = 0.$$

(2)

Introducing (λ) as a linear scale factor, the governing equations may be combined in one equation as follows:

$$\lambda\left(\frac{dV}{dt} + \frac{1}{\rho}\frac{\partial P}{\partial s} + g\frac{dz}{ds} + \frac{f}{2D}V|V|\right) + a^2\frac{\partial V}{\partial s} + \frac{1}{\rho}\frac{dP}{dt} = 0.$$

(3)

By breaking the terms (dV/dt) and (dP/dt) down into their components and regrouping terms, the equation becomes:

$$\left(\lambda\frac{\partial V}{\partial t} + (\lambda V + a^2)\frac{\partial V}{\partial s}\right) + \left(\frac{1}{\rho}\frac{\partial P}{\partial t} + (\frac{V}{\rho} + \frac{\lambda}{\rho})\frac{\partial P}{\partial s}\right)$$
$$+ \lambda g\frac{dz}{ds} + \frac{\lambda f}{2D}V|V| = 0.$$

(4)

Some manipulations are then performed to this equation to replace the original two partial differential equations with two ordinary differential equations as follows:

$$\frac{dV}{dt} + \frac{g}{a}\frac{dH}{dt} - \frac{g}{a}V\frac{dz}{ds} + \frac{f}{2D}V|V| = 0 \qquad \text{for}$$

$$\frac{ds}{dt} = V + a, \quad \text{and}$$

(5)

$$\frac{dV}{dt} - \frac{g}{a}\frac{dH}{dt} + \frac{g}{a}V\frac{dz}{ds} + \frac{f}{2D}V|V| = 0 \qquad \text{for}$$

$$\frac{ds}{dt} = V - a.$$

(6)

Where the pressure (P) was replaced by its equivalent term $\rho g(H-z)$.

Eq. (5) is usually known as the C^+ characteristic equation while eq. (6) is known as the C^- characteristic equation. Eqs. (5, 6) can now be expressed in a finite difference form, as follows:

The C^+ equation becomes;

$$\frac{V_P - V_L}{\Delta t} + \frac{g}{a}\frac{H_P - H_L}{\Delta t} - \frac{g}{a}V_L\frac{dz}{ds} + \frac{fV_L|V_L|}{2D} = 0.$$

(7)

The C^- equation becomes;

$$\frac{V_P - V_R}{\Delta t} - \frac{g}{a}\frac{H_P - H_R}{\Delta t} + \frac{g}{a}V_R\frac{dz}{ds} + \frac{fV_R|V_R|}{2D} = 0.$$

(8)

In applying the finite difference numerical analysis, the pipe has to be divided into a number of sections. Grid points along the s-axis represent points are spaced (Δs) apart along the pipe.

3.2. Modeling the viscoelastic behavior of the pipe walls

The viscoelasticity of the pipe walls are modeled using a Kelvin-Voigt model. For

simplicity, a Kelvin-Voigt model with only one element will be introduced into the continuity equation, eq. (1). The modified continuity equation will take the following form [17]:

$$\frac{dH}{dt} + \frac{a^2}{g}\frac{\partial V}{\partial s} + 2\frac{a^2}{g}\frac{d\varepsilon_1}{dt} = 0. \tag{9}$$

Where,

$$\frac{d\varepsilon_1}{dt} = \frac{1}{\tau_1}\left(\frac{PD\lambda}{2eE_1} - \varepsilon_1\right). \tag{10}$$

By substituting from eq. (10) into eq. (9), one gets:

$$\frac{dH}{dt} + \frac{a^2}{g}\frac{\partial V}{\partial s} + 2\frac{a^2}{g}\frac{1}{\tau_1}\left(\frac{PD\lambda}{2eE_1} - \varepsilon_1\right) = 0. \tag{11}$$

Where; D is the pipe diameter, e is the pipe wall thickness, $\tau_1 = \frac{\eta_1}{E_1}$ is the retardation time, η_1 is the viscosity of the generic element, E_1 is the modulus of elasticity of the generic element, and λ is the constraint coefficient in the wave-speed formula.

Hence, an additional term appeared in the continuity equation to account for the viscoelastic behavior of the pipe walls as given in eq. (11).

When eq. (11) is solved with the momentum equation by the MOC, following the same procedure as in section (3.1), the following characteristic equations are obtained in which the dominant effect of this viscoelastic nature is clearly recognized.

$$C^+: V_P - V_L + \frac{g}{a}(H_P - H_L) - \frac{g\Delta t}{a}V_L\frac{dz}{ds} + gh_{fL}\Delta t$$
$$+ \frac{2a\Delta t}{\tau_1}\left(\frac{\rho gH_LD\lambda}{2eE_1} - \varepsilon_{1L}{}^{t-\Delta t}\right) = 0, \tag{12}$$

$$C^-: V_P - V_R - \frac{g}{a}(H_P - H_R) + \frac{g\Delta t}{a}V_R\frac{dz}{ds} + gh_{fR}\Delta t$$
$$+ \frac{2a\Delta t}{\tau_1}\left(\frac{\rho gH_RD\lambda}{2eE_1} - \varepsilon_{1R}{}^{t-\Delta t}\right) = 0. \tag{13}$$

The values of the retarded strain $\varepsilon_{1L}{}^t$ and $\varepsilon_{1R}{}^t$ could be computed at each time step from the following equations, obtained from eq. (10):

$$\frac{\varepsilon_{1L}{}^t - \varepsilon_{1L}{}^{t-\Delta t}}{dt} = \frac{1}{\tau_1}\left(\frac{\rho gH_LD\lambda}{2eE_1} - \varepsilon_{1L}{}^{t-\Delta t}\right), \tag{14}$$

and

$$\frac{\varepsilon_{1R}{}^t - \varepsilon_{1R}{}^{t-\Delta t}}{dt} = \frac{1}{\tau_1}\left(\frac{\rho gH_RD\lambda}{2eE_1} - \varepsilon_{1R}{}^{t-\Delta t}\right). \tag{15}$$

3.3. Modeling unsteady friction

The unsteady friction terms (h_{fL} and h_{fR}) in eqs. (12,13) are accurately modeled by the universal model presented by Warda et al.. [13] which is a modification of Vardy et al.'s model. The original model of Vardy et al. is suitable for turbulent flows, while an adjustment was introduced for laminar flows. The governing equations are:

$$h_{fL}(K\Delta t) = \frac{fV_L(i, K\Delta t)|V_L(i, K\Delta t)|}{4gR}$$
$$+ \frac{4\nu}{gR^2}\sum_{J=1}^{K}\left[V_L((i, K-J+1)\Delta t) - V_L((i, K-J)\Delta t)\right]$$
$$W\left[\left(J-\frac{1}{2}\right)\Delta t\right], \tag{16}$$

$$h_{fR}(K\Delta t) = \frac{fV_R(i, K\Delta t)|V_R(i, K\Delta t)|}{4gR}$$
$$+ \frac{4\nu}{gR^2}\sum_{J=1}^{K}\left[V_R((i, K-J+1)\Delta t) - V_R((i, K-J)\Delta t)\right]$$
$$W\left[\left(J-\frac{1}{2}\right)\Delta t\right], \tag{17}$$

$$\overline{W}(\tau) = W(t) = \left(\frac{1}{2\sqrt{\pi\tau}}\right)e^{-\tau/C^*}. \tag{18}$$

Where;

C^* is the shear decay coefficient $= \dfrac{7.41}{R_N{}^b}$ (19)

and the exponent, b, is given by:

$$b = \log_{10}\left(\frac{14.3}{R_N^{0.05}}\right). \qquad (20)$$

For laminar flow, the value of the shear decay coefficient takes a constant value, irrespective of Reynolds Number, Warda et al. [13] suggested a suitable value as:

$$C^* = 0.0215. \qquad (21)$$

By solving the set of equations from (12) to (21), the numerical model can deal with unsteady friction and the viscoelastic behavior of the pipe walls in transient problems.

The numerical model was verified against laminar and turbulent flow experimental data to examine its efficiency and accuracy in simulating the pressure transients in viscoelastic pipes as presented by Warda et al. [17].

4. Models of column separation

Two approaches are considered for modeling column separation, namely the Discrete Vapor Cavity Model (DVCM) and the Discrete Gas Cavity Model (DGCM).

4.1. The discrete vapor cavity model (DVCM)

4.1.1. The standard DVCM

The model allows vapor cavities to form at the computational sections in the MOC. A constant wave speed is assumed for the liquid between computational sections. As long as the pressure at the computational section is greater than the liquid vapor pressure, the solution by the method of characteristics is unaltered.

When the pressure at a computational section (P) drops below the vapor pressure of the liquid, the solution by the method of characteristics is no longer valid. The pressure at that section is then set to the vapor pressure and a vapor cavity is assumed to occur.

$$H_p = H_v, \qquad (22)$$

where H_v is the liquid vapor pressure, dependent on the liquid temperature.

The characteristic eqs. (12, 13) are then utilized to compute the upstream velocity (V_{pu}) and the downstream velocity (V_{pd}) at the computational section (P).

$$C^+; \ V_{Pu} - V_L + \frac{g}{a}(H_P - H_L) - \frac{g\Delta t}{a}V_L\frac{dz}{ds} + gh_{fL}\Delta t$$
$$+ \frac{2a\Delta t}{\tau_1}\left(\frac{\rho g H_L D\lambda}{2eE_1} - \varepsilon_{1L}^{t-\Delta t}\right) = 0, \qquad (23)$$

$$C-; \ V_{Pd} - V_R - \frac{g}{a}(H_P - H_R) + \frac{g\Delta t}{a}V_R\frac{dz}{ds} + gh_{fR}\Delta t$$
$$+ \frac{2a\Delta t}{\tau_1}\left(\frac{\rho g H_R D\lambda}{2eE_1} - \varepsilon_{1R}^{t-\Delta t}\right) = 0. \qquad (24)$$

The vapor cavity volume could now be calculated from the following continuity equation

$$C.E.; \ \Delta\forall_v = \int_{t-\Delta t}^{t} A\left(V_{pd} - V_{pu}\right)dt, \qquad (25)$$

where, A is the pipe cross-sectional area and $\forall_v$ is the vapor cavity volume.

The solution of the continuity equation for the vapor cavity volume is given by Wylie [25] as follows:

$$\left(\forall_v\right)_t = \left(\forall_v\right)_{t-\Delta t} + A\{(1-\psi)\left[\left(V_{pd}\right)_{t-\Delta t} - \left(V_{pu}\right)_{t-\Delta t}\right]$$
$$+ \psi\left[\left(V_{pd}\right)_t - \left(V_{pu}\right)_t\right]\}\Delta t. \qquad (26)$$

Eq. (26) integrates the continuity equation of the vapor cavity volume using a weighting factor (ψ) in the time direction. The weighting factor can take any value in the range between 0.0 and 1.0. A practical range between 0.5 and 1.0 was recommended by Simpson and Bergant [19]. The standard form for eq. (26) usually uses a value of ($\psi = 0.5$).

Eqs. (22-24, 26) are the main equations for the DVCM and continue to be applied as long as the vapor cavity volume is a positive value. When a negative vapor cavity volume is

calculated from eq. (26), this implies that the cavity has collapsed and the solution by the method of characteristics is reinstated.

However, the DVCM generates unrealistic pressure spikes due to the collapse of multicavities, Wylie [22]. An attempt to overcome this problem was introduced by Safwat and van der Polder [20].

4.1.2. DVCM modification by Safwat and Van Der Polder

Safwat and Van Der Polder [20] allowed discrete vapor cavities to form only at predetermined locations (e.g., at valves and high points). At these locations, the given equations for the DVCM are unchanged. However, if the pressure drops below the vapor pressure at a computational section where discrete vapor cavities are not allowed to form, an alternative procedure is applied.

In this procedure, the pressure at the computational section is set to the vapor pressure ($H_P = H_v$). The upstream and downstream velocities are calculated at that section from eqs. (23 , 24). To prevent column separation (formation of a vapor cavity) at that section, the upstream and downstream velocities must be the same. Therefore, an average flow velocity is estimated at that section through the following equation:

$$\overline{V_P} = \frac{V_{pu} + V_{pd}}{2}.$$

4.1.3. Verification of the DVCM

The DVCM with ($\psi = 0.5$) is now embedded into the modified MOC model. The modification proposed by Safwat and van der Polder is applied by allowing the formation of vapor cavities at the solenoid valve only. The results of the modified model are now verified through an experimental flow case ($R_N = 57150$) in which column separation was present. Results of the comparison are shown in fig. 2.

Fig. 2 shows that there is no agreement in phase between the numerical and experimental results. The disagreement in phase may be attributed to the air release phenomenon that usually accompanies column separation. Air release is well known to effectively decrease the wave speed. This is

shown through the experimental data where the wave speed is clearly altered after the first cavity collapse. It is concluded that the DVCM is incapable of simulating the air release phenomenon. It is proposed that the air release phenomenon could be simulated if the DGCM is applied instead of the DVCM.

4.2. The discrete gas cavity model (DGCM)

In the DGCM, discrete gas cavities replace discrete vapor cavities at the computational sections. Between the computational sections, liquid is assumed to exist without free gas. In other words, the DGCM lumps the mass of free gas at the computing sections. Each gas cavity is assumed to expand and contract isothermally as the pressure varies according to the perfect gas equation of state. Fig. 3 gives a simple representation of the DGCM.
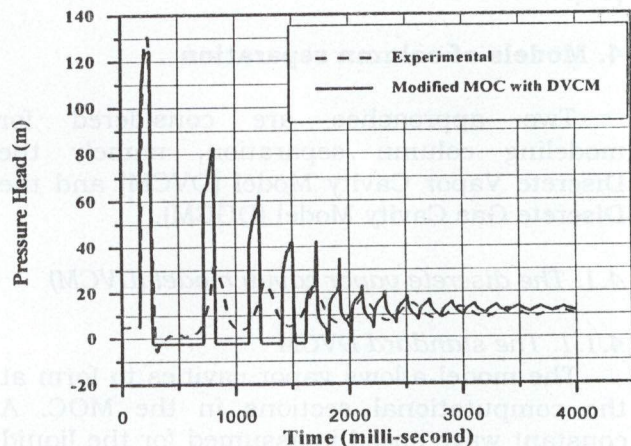

Fig. 2. Predicted pressure time history by the modified MOC with the DVCM, R_N=57150.

The DGCM described using eqs. (27) through (29), which replace eqs. (23), 24 and (26), respectively.

$$C^+; V_{Pu} - V_L + \frac{g}{a}(H_P - H_L) - \frac{g\Delta t}{a}V_L\frac{dz}{ds} + gh_{fL}\Delta t$$
$$+ \frac{2a\Delta t}{\tau_1}\left(\frac{\rho g H_L D\lambda}{2eE_1} - \varepsilon_{1L}^{t-\Delta t}\right) = 0, \tag{27}$$
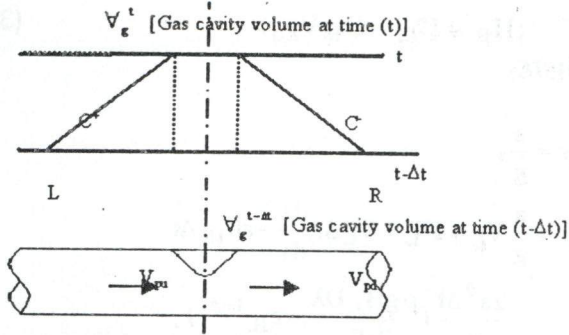
Fig. 3. Representation of the DGCM.

$$C^{-} \; ; \; V_{Pd} - V_R - \frac{g}{a}(H_P - H_R) + \frac{g\Delta t}{a} V_R \frac{dz}{ds} + gh_{fR}\Delta t$$

$$+ \frac{2a\Delta t}{\tau_1}\left(\frac{\rho g H_R D\lambda}{2eE_1} - \varepsilon_{1R}{}^{t-\Delta t}\right) = 0 , \qquad (28)$$

$$C.E.; \; \left(\forall_g\right)_t = \left(\forall_g\right)_{t-\Delta t} + A\left\{(1-\psi)\left[\left(V_{pd}\right)_{t-\Delta t} - \left(V_{pu}\right)_{t-\Delta t}\right]+\right.$$

$$\left. \psi\left[\left(V_{pd}\right)_t - \left(V_{pu}\right)_t\right]\right\}\Delta t . \qquad (29)$$

Perfect gas equation of state:

$$M_g R_g T = P_g{}^{*}\alpha\forall = P_0{}^{*}\alpha_0\forall . \qquad (30)$$

Where:

$\forall$ = Volume of the liquid-gas mixture
α_0 = Void fraction at a reference pressure $P_0{}^{*}$
$P_g{}^{*}$ = Absolute gas pressure

A relation is obtained between (H_p) and the absolute gas pressure $(P_g{}^{*})$ from fig. 4 in the following form:

$$P_g{}^{*} = \rho_L g\left(H_p - Z - H_v\right) . \qquad (31)$$

By substituting from eq. (31) into eq. (30), the following equation is obtained:

$$\forall_g{}^{t} = \frac{P_0{}^{*}\alpha_0\forall}{\rho_L g\left(H - Z - H_v\right)} . \qquad (32)$$

By defining a constant (C_1) as:

$$C_1 = \frac{P_0{}^{*}\alpha_0\forall}{\rho_L g} , \qquad (33)$$

eq. (29) could be reduced to the following form:

$$\forall_g{}^{t} = \frac{C_1}{\left(H_p - Z - H_v\right)} \qquad (34)$$

Eq. (34) represents the relation between (H_p) and the absolute gas pressure $(P_g{}^{*})$. By solving eqs. (27, 28, 29, 33, 34) simultaneously, the column separation phenomenon and the effect of air release on the pressure transient could be efficiently simulated.
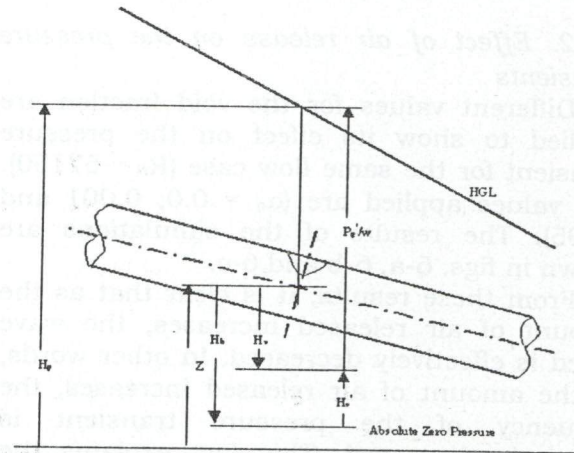

Fig. 4. The relation between (H_p) and the absolute gas pressure $(P_g{}^{*})$.

4.2.1. Verification of the DGCM

The modified MOC including the DGCM is now verified through an experimental flow case (R_N = 57150) in which column separation is present. A void fraction (α_0= 0.0026) at a reference pressure (P_0= 1.013 bar) is assumed at all nodes. The pipe is discretized into four parts. Results of the comparison are shown in fig. 5.
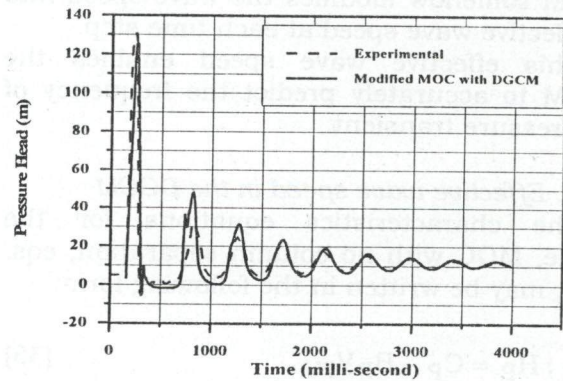

Fig. 5. Modified MOC with DGCM vs. experimental data, R_N=57150.

Fig. 5 shows that column separation could be accurately simulated by the DGCM. By comparing figs. 2 and 5, it is noted that the main factor controlling the frequency of the pressure transient is the amount of air released during the column separation phenomenon. A demonstration of the effect of air release on the pressure transient is presented in the next section by applying different values for the void fraction.

4.2.2. Effect of air release on the pressure transients

Different values for the void fraction are applied to show its effect on the pressure transient for the same flow case ($R_N = 57150$). The values applied are ($\alpha_o = 0.0$, 0.001 and 0.005). The results of the simulations are shown in figs. 6-a, 6-b and 6-c.

From these results, it is clear that as the amount of air released increases, the wave speed is effectively decreased. In other words, as the amount of air released increases, the frequency of the pressure transient is effectively decreased. This fact explains the inaccuracy of the DVCM in modeling column separation when accompanied by air release, as the DVCM is incapable of simulating the effect of air release on the pressure transient.

It is also shown that the magnitude of the pressure peak resulting from the collapse of the first cavity is significantly reduced when a larger amount of air is released.

The capability of the DGCM to predict the effect of the void fraction on the frequency of the pressure transient, while maintaining a constant wave speed (a), indicates that the DGCM somehow modifies the wave speed into an effective wave speed at each time step.

This effective wave speed enables the DGCM to accurately predict the frequency of the pressure transient.

4.2.3. Effective wave speed in the DGCM

The characteristics equations for the simple, MOC with no column separation, eqs. (7, 8), may be written in the following form:

$$C^+ \quad ; H_P = C_P - B_P V_{PU}, \qquad (35)$$

and

$$C^- \quad ; H_P = C_M - B_M V_{Pd}. \qquad (36)$$

Where:

$$B_P = \frac{a}{g},$$

$$C_P = \frac{a}{g} V_L + H_L + V_L \Delta t \frac{dz}{ds} - ah_{fR} \Delta t$$
$$- \frac{2a^2 \Delta t}{g\tau_1} \left(\frac{\rho g H_L D\lambda}{2eE_1} - \varepsilon_{1L}^{t-\Delta t} \right),$$

$$B_M = \frac{a}{g}, \text{ and}$$

$$C_M = -\frac{a}{g} V_R + H_R + V_R \Delta t \frac{dz}{ds} + ah_{fR} \Delta t$$
$$- \frac{2a^2 \Delta t}{g\tau_1} \left(\frac{\rho g H_R D\lambda}{2eE_1} - \varepsilon_{1R}^{t-\Delta t} \right).$$

Simultaneous solution of the characteristic eqs. (35, 36) gives:

$$H_p = \frac{1}{2}(C_P + C_M) - \frac{a}{2g}\left(V_{pu}^t - V_{pd}^t \right). \qquad (37)$$

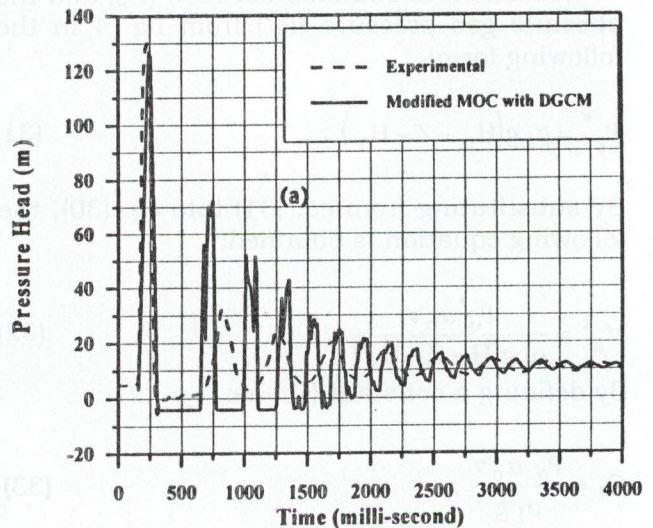The final solution for the governing equations of the DGCM, eqs. (27, 28), takes the following form:

Fig. 6-a. Effect of air release at different values of void fraction, $\alpha_o = 0.0$.
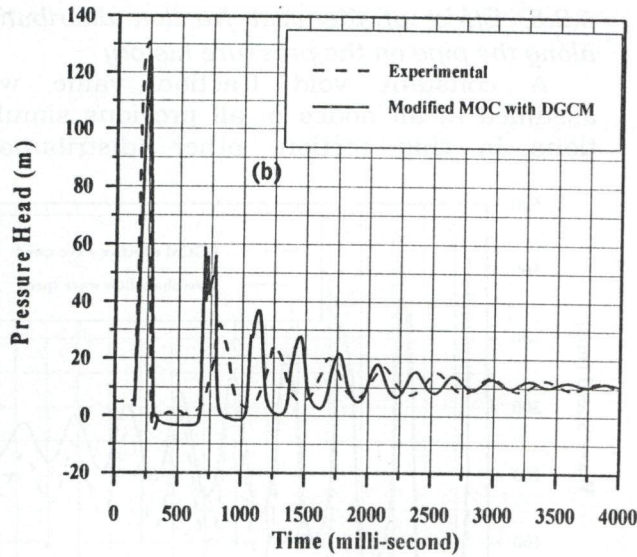
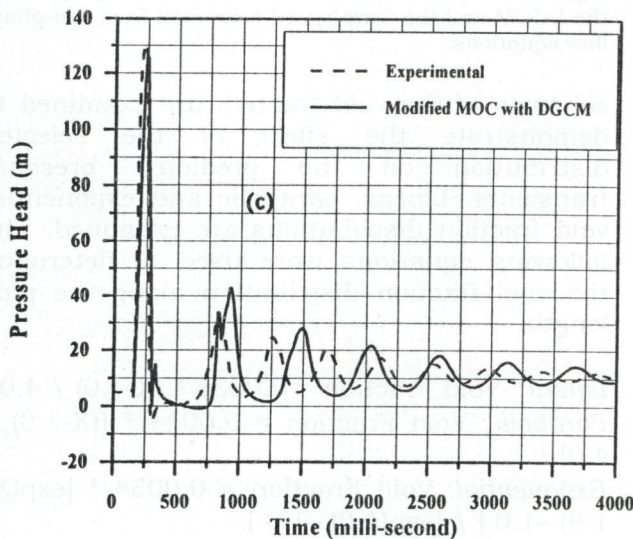Fig. 6-b. Effect of air release at different values of void fraction, α_o = 0.001.

Fig. 6-c. Effect of air release at different values of void fraction, α_o = 0.005.

$$H_P - Z - H_v = -B_1(1 + \sqrt{1 + \frac{C_4}{B_1^2}}) \quad \text{if } B_1 < 0, \quad (38)$$

$$H_P - Z - H_v = -B_1(1 - \sqrt{1 + \frac{C_4}{B_1^2}}) \quad \text{if } B_1 > 0. \quad (39)$$

Where:

$$C_4 = \frac{B_M B_P C_1}{A\psi \, \Delta t(B_M + B_P)},$$

$$B_1 = 0.5\,[B_M B_P B_2 B_V + (Z + H_V) - B_2(C_P B_M + C_M B_P)],$$

$$B_2 = \frac{1}{B_M + B_P},$$

and

$$B_V = \frac{\forall_g^{t-\Delta t}}{A\psi \, \Delta t} + \frac{1-\psi}{\psi}(V_{Pd}^{t-\Delta t} - V_{Pu}^{t-\Delta t}).$$

To develop an expression for the effective wave speed in the DGCM, eqs. (38, 39) are solved simultaneously and the solution takes the form:

$$H_p(2\beta \pm 1) = \frac{\beta}{2}(C_P + C_M) - \frac{a\beta}{2g}\left(V_{pu}{}^t - V_{pd}{}^t\right)$$
$$+ (\beta \pm 1)(Z + H_v) - \frac{a\beta}{2g}\frac{(\forall_g)^t}{A\psi\Delta t}. \quad (40)$$

Where:

$$\beta = \sqrt{\frac{0.5\psi}{2\psi B_1{}^2 \frac{\rho_L{}^2 g^2}{P_g^{*2}} + \frac{\rho_L \alpha a^2}{P_g^*}}}. \quad (41)$$

The similarity between eq. (40) for column separation and eq. (37) for no column separation is clear, and it is shown that in the DGCM, eq. (40), two extra terms are present and also the wave speed is always multiplied by a factor (β) resulting in an effective wave speed:

$$a_{eff} = a\beta,$$

$$a_{eff} = a\sqrt{\frac{0.5\psi}{2\psi B_1{}^2 \frac{\rho_L{}^2 g^2}{P_g^{*2}} + \frac{\rho_L \alpha a^2}{P_g^*}}} \quad (42)$$

Eq. (42) shows a very important fact. This fact is that although the wave speed is constant value input in the DGCM, however the DGCM modifies this value into an effective wave speed (a_{eff}) using eq. (42) at each time

step. This enables the DGCM to predict the effect of the void fraction and the pressure on the value of the wave speed at each time step and consequently on the frequency of the pressure transient.

This result is verified by first considering the case with ($\alpha = 0$) and also by comparison with the two-phase model as presented in the next section.

It can be shown that at ($\alpha = 0$), the solution of the DGCM, eq. (40), and that of the simple MOC, eq. (37), are identical and the wave speed in the DGCM remains unaltered because β is equal to unity at $\alpha = 0$.

4.2.4. Wave speed equation for two phase flow

Wylie [2] gave an expression for the wave speed in two-phase flow transients for low void fractions:

$$a_{two\ phase} = a \sqrt{\frac{1}{1 + \dfrac{\rho_L \alpha a^2}{P_g^*}}}.$$

By comparing this equation with the equation for the effective wave speed in the DGCM:

$$a_{eff} = a \sqrt{\frac{0.5\psi}{2\psi B_1^2 \dfrac{\rho_L^2 g^2}{P_g^{*2}} + \dfrac{\rho_L \alpha a^2}{P_g^*}}}$$

A clear resemblance is noticed between the two equations. However, to further clarify the comparison between the two equations, both equations are used to estimate the variable wave speed at the valve for the experimental test case ($R_N=57150$). The results of both equations are compared through fig. 7.

The comparison shows that the effective wave speed predicted by the DGCM matches closely with the wave speed estimated from two phase flow equations. This gives more confidence in the usage of the DGCM in the analysis of single phase flow transients accompanied by air release and also in the analysis of two phase flow transients with low void fractions.

4.2.5. Effect of the void fraction distribution along the pipe on the pressure history

A constant void fraction value was assumed at all nodes in all previous simulations. In this section, other distribution
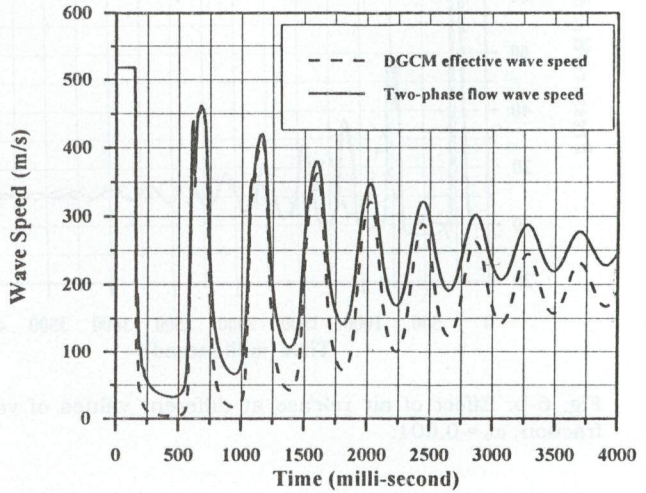

Fig. 7. A comparison between the effective wave speed for the DGCM and the wave speed estimated from two-phase flow equations.

schemes of the void fraction are examined to demonstrate the effect of the selected distribution on the predicted pressure transients. Linear, parabolic and exponential void fraction distributions are examined. The following equations were used to determine the void fraction distribution along the pipe length.

Linear: Void Fraction = 0.0036 * (X-1.0) / 4.0,
Parabolic: Void Fraction = 0.0044 * [(X-1.0) / 4.0] ^{2},
Exponential: Void Fraction = 0.0054 * [exp(X-1.0) −1.0] / [exp(4.0) −1.0].

Where X is a dimensionless parameter that varies from 1.0 at the pipe inlet to 5.0 at the pipe exit. The results of the three void fraction distributions are shown in figs. 8-a, 8-b and 8-c.

From the previous figures, it is clearly shown that a constant distribution of the void fraction along the pipe is more accurate than all other proposed distributions.

These results indicate that when a low-pressure transient occurs, air is released

uniformly at all points and is not concentrated at the cavity region. Moreover, assuming uniform release of air along the pipe simplifies the application of the DGCM by selecting a single value for the void fraction for all nodes, without the need for selecting any void fraction distribution.
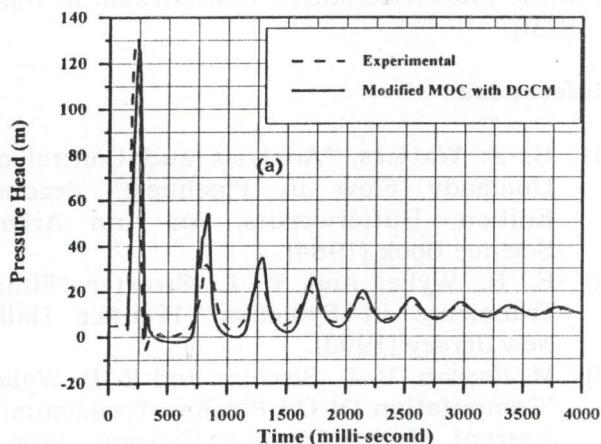

Fig. 8-a. Predicted pressure transient based on void fraction distribution, linear.

5. Conclusions

A numerical model based on the MOC was developed for modeling pressure transients in viscoelastic pipelines. The model is capable of dealing with column separation, unsteady friction and the viscoelastic behavior of the pipe walls.
1) The DVCM proved to be incapable of simulating column separation when the column separation is accompanied by air release.
This study showed that the DGCM is capable of simulating the column separation efficiently at much higher void fractions than those reported by Simpson and Bergant [19].
2) A constant void along the pipeline provided the best numerical simulation of the experimental test case. This implies that during low-pressure transients, air is released uniformly along the pipe and is not concentrated at the region of the cavity only.
3) The disadvantages of the DGCM are the determination of a suitable value for the void fraction and the increased complexity of programming.

An expression for the effective wave speed in the DGCM is developed. This expression shows the mechanism that enables the DGCM to predict the frequency of the transient.
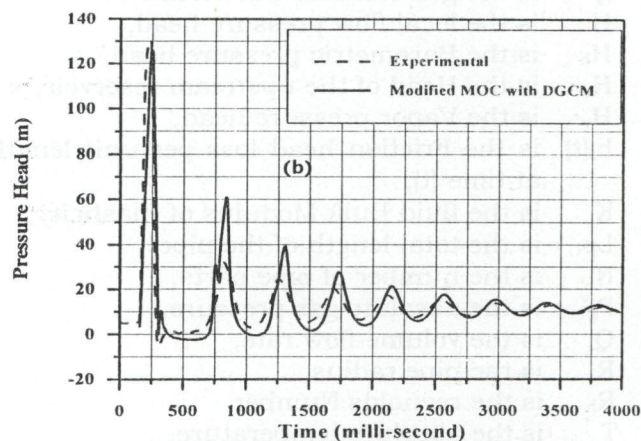

Fig. 8-b. Predicted pressure transient based on void fraction distribution, parabolic.
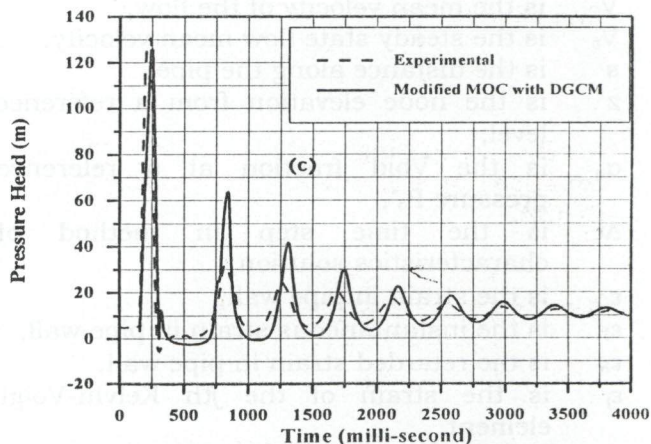

Fig. 8-c. Predicted pressure transient based on void fraction distribution, exponential.

Nomenclature

A	is the cross-sectional area of the flow,
a	is the ave speed in a fluid contained within an elastic conduit,
a_o	is the wave speed in a rigid pipe,
a_{eff}	is the effective wave speed in the DGCM,
C^+	is the characteristic curve, transmitting information downstream,
C^-	is the characteristic curve, transmitting information upstream,
D	is the pipe diameter,
E	is the young's Modulus of Elasticity for the pipe material,

E_j is the modulus of Elasticity of the jth Kelvin-Voigt element,

e is the pipe wall thickness,

f is the darcy-Weisbach friction factor,

g is the gravitational acceleration ,

H is the local flow pressure head,

H_b is the Barometric pressure head,

H_o is the Head of the upstream reservoir,

H_v is the Vapor pressure head,

$h_f(t)$ is the Friction head loss per unit length at time (t),

K is the fluid Bulk Modulus of Elasticity,

Lp is the total length of the pipe,

N is the number of pipe parts,

P_g^* is the absolute gas pressure,

Q is the volume flow rate,

R is the pipe radius,

R_N is the reynolds Number,

T is the absolute temperature,

t is the time,

T_c is the valve closure time,

V is the mean velocity of the flow,

V_o is the steady state flow mean velocity,

s is the distance along the pipe,

z is the node elevation from a reference level,

α_o is the Void fraction at a reference pressure P_o^*,

Δt is the time step in method of characteristics solution,

ε is the strain in pipe wall,

ε_I is the instantaneous strain in pipe wall,

ε_R is the retarded strain in pipe wall,

ε_j is the strain of the jth Kelvin-Voigt element,

ψ is the weighting factor used in the DVCM and DGCM,

λ is the constraint coefficient in the wave speed formula, also used as the multiplier in the solution by the method of characteristics,

ν is the fluid kinematic viscosity,

ρ is the fluid density,

σ is the stress at the pipe wall,

τ is the Dimensionless time in the unsteady friction models,

τ_j is the retardation time of the jth Kelvin-Voigt element,

η_j is the viscosity of the jth Kelvin-Voigt element,

$\forall$ is the volume of the liquid-gas mixture,

$\forall_v$ is the vapor cavity volume, and

$\forall_g$ is the gas cavity volume.

Subscripts

P is the node to be calculated at time (t),

R is the known condition upstream at time (t-Δt), and

L is the known condition downstream at time (t-Δt).

References

[1] G. Z. Watters, "Analysis and Control of Unsteady Flow in Pipelines," Second Edition, Butterworths, An Ann Arbor Science Book (1984).

[2] E. B. Wylie, and V. L. Streeter "Fluid Transients in Systems," Prentice Hall, New Jersey (1993).

[3] M. Kaplan, V. L. Streeter and E. B. Wylie "Computation Of Oil Pipeline Transients," Journal of the Pipeline Division, Proc., ASCE, Vol. 93 (PL3), (1967).

[4] A. Bergant, and A. Simpson, "Quadratic Equation Inaccuracy For Water Hammer," Journal of Hydraulic Engineering, Vol. 117 (11), (1991).

[5] P. F. Boulos, D. J. Wood and J. E. Funk, "A Comparison Of Numerical And Exact Solutions For Pressure Surge Analysis", Proc., 6th International Conference on Pressure Surges, British Hydromechanics Research Association (BHRA), Cranfield, U.K., pp. 149-160 (1990).

[6] W. Zielke, "Frequency-Dependent Friction In Transient Pipe Flow," Journal Of Basic Engineering, Trans. ASME, Vol. 90 (1), pp. 109-115 (1968).

[7] A. E. Vardy, and K. L. Hwang, "A Characteristics Model Of Transient Friction In Pipes," Journal of Hydraulic Research, Vol. 29 (5), pp. 669-684 (1991).

[8] B. Brunone, U. M. Golia, and M. Greco, "Some Remarks On The Momentum Equation For Fast Transients," Proc., International Conference On Hydraulic Transients With Water Column Separation, IAHR, Valencia, Spain, pp. 201-209 (1991).

[9] A. K. Trikha, "An Efficient Method For Simulating Frequency-Dependent Friction In Transient Liquid Flow," Journal of

Fluids Engineering, Trans. ASME, Vol. 97 (1), pp. 97-105 (1975).

[10] K. Suzuki, T. Taketomi and S. Sato, "Improving Zielke's Method Of Simulating Frequency-Dependent Friction In Laminar Liquid Pipe Flow," Journal of Fluids Engineering, Vol. 113, pp.569-573 (1991).

[11] A. E. Vardy and J. Brown, "Transient, Turbulent, Smooth Pipe Friction," Journal of Hydraulic Research, Vol. 33 (4), pp. 435-456 (1995).

[12] B. Brunone, U. M. Golia, and M. Greco, "Effects Of Two-Dimensionality On Pipe Transients Modeling," Journal of Hydraulic Engineering, Vol. 121 (12), pp. 906-912 (1995).

[13] H. A. Warda, H. A. Kandil, A. A. Elmiligui and E. M. Wahba, "Modeling Unsteady Friction in Rapid Transient Pipe Flows ," Vol. 40 (5),pp. 783-795 (2001).

[14] L. Suo and E. B. Wylie, "Complex Wave Speed And Hydraulic Transients In Viscoelastic Pipes," J. of Fluids Engineering, Trans. ASME, Vol. 112, pp. 496-500 (1990).

[15] M. S. Guney, "Water hammer In Viscoelastic Pipes Where Cross-Section Parameters Are Time Dependent," Proc., 4th International Conference on Pressure Surges, British Hydromechanics Research Association (BHRA), Cranfield, U.K., pp. 189-204 (1983).

[16] G. Pezzinga and P. Scandura, "Unsteady Flow In Installations With Polymeric Additional Pipe," Journal of Hydraulic Engineering, Vol. 121 (11), pp. 802-811 (1995).

[17] H. A. Warda, H. A. Kandil, A. A. Elmiligui and E. M. Wahba, "Modeling Pressure Transients in Viscoelastic Pipes," ASME, PVP Conference, GA, USA (2001).

[18] J. A. Swaffield and A. P. Boldy, "Pressure Surges in Pipe and Duct Systems," Avebury Technical, Ashgate Publishing Ltd (1993).

[19] A. Simpson and A. Bergant, "Numerical Comparison Of Pipe-Column-Separation Models," Journal of Hydraulic Engineering, Vol. 120 (3), pp. 361-377 (1994).

[20] H. H. Safwat and van der J. Polder, "Experimental And Analytic Data Correlation Study Of Water Column Separation," Journal of Fluids Engineering, Vol. 94 (1), pp. 91-97 (1973).

[21] G.A. Provoost and E.B. Wylie, "Discrete gas mode to represent distributed free gas in liquids" Proc. 5th Int. symp. On Column Separation, International Association of Hydraulic Research, the Netherlands, pp. 249-258 (1981).

[22] E. B. Wylie, "Simulation Of Vaporous And Gaseous Cavitation," Journal of Fluids Engineering, Transactions of the ASME, Vol. 106 (3), pp. 307-311 (1984).

[23] W. Rongqiso and L. Youhus, "Numerical Analysis For Transient Cavitation And Column Separation," Wuhan, China (1988).

[24] J. Aga, T. J. Karterud and T. K. Nielsen, "Testing Of Transient Flow And Column Separation In Crude Oil Pipelines," Proc., 3rd Int. Conference on Pressure Surges, British Hydromechanics Research Association (BHRA), Cranfield, U.K., pp. 113-126 (1980).

[25] V. L. Streeter, "Transient Cavitating Pipe Flow," Journal of Hydraulic Engineering, Vol. 109 (11) (1983).

[26] A. Simpson and E. B. Wylie, "Large Water-Hammer Pressures For Column Separation In Pipelines," Journal of Hydraulic Engineering, Vol. 117 (10), pp. 1310-1316 (1991).

Alexandria Engineering Journal. Vol. 41, No. 2, March 2002

203